MJFAS MALAYSIAN JOURNAL OF FUNDAMENTAL AND APPLIED SCIENCES
PRINT ISSN: 2289-5981 | ONLINE ISSN: 2289-599X

FULL PAPER

Multiplication gain and excess noise factor in thin SiC avalanche photodiodes

Cha Chee Sun, Ah Heng You *

Faculty of Engineering and Technology, Multimedia University, Jalan Ayer Keroh Lama, 75450 Melaka, Malaysia

* *Corresponding author: ahyou@mmu.edu.my*

Article history
Received 29 July 2016
Accepted 16 October 2016

Graphical abstract

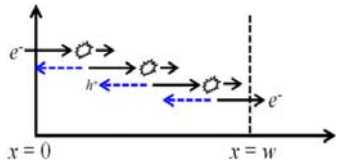

Abstract

This work simulated the avalanche characteristics of 4H- and 6H-SiC avalanche photodiodes (APDs) at 0.1 μm, 0.2 μm and 0.3 μm avalanche widths. A Monte Carlo model with random ionization path length techniques is developed to simulate mean multiplication gain and excess noise factor in thin SiC APDs. Mean multiplication gain, breakdown voltage and excess noise factor are simulated based on the electric field dependent impact ionization coefficients with the inclusion of dead space effect. Our results show that hole-initiated impact ionization gives high multiplication gain with low excess noise factor in both devices. We observed that dead space effect is more pronounce in thin structure since it covers a significant portion of the avalanche region. In thick device structure, a high breakdown voltage is observed. A comparison between these two polytypes shows that 4H-SiC provides high multiplication gain with low excess noise factor than 6H-SiC.

Keywords: Silicon carbide (SiC), avalanche photodiode, impact ionization, dead space, multiplication gain, excess noise factor

INTRODUCTION

Silicon (Si) had been long being used as the main material in the fabrication of many electronics devices. The intrinsic material properties of Si had becomes a limitation in the emerging of technology advances towards a high power and high frequency applications under elevated temperature. III-nitride semiconductor has appeared to be one of the alternative materials for replacing Si in the design of photodetector devices [1 – 3]. However, this material suffers from a large dark current being observed at the breakdown edge [4, 5]. The lack of III-nitride nature substrate had further discouraged the choices in the fabrication of device application. Among other wide band gap materials, silicon carbide (SiC) has received extensive attention in recent years due to its superior physical properties [6 – 8]. With the capability of poses a high breakdown electric field, high saturated drift velocity and relatively high thermal conductivity, SiC had become an attractive material in realizing high temperature, high frequency and high power devices. It also had been proven to be a potential alternative to III-nitride based avalanche photodiode (APD) for UV detection [9, 10].

The performance of an APD can be determined from the multiplication gain and excess noise factor that arise from the chain process of impact ionization. Multiplication gain plays a very important role as an internal gain of APD which will amplify the weak incoming photo electric signal to a greater value for further device processing. However, multiplication gain is always affected by the presence of excess noise factor due to the stochastic process of impact ionization which can cause a significant deterioration to the overall APD performance. Loh *et al.* (2008) measured the multiplication characteristics in thick 4H-SiC APD structures by using 244nm and 325nm UV light. They observed a high multiplication gain using 244nm illuminating light. Their results show an increasing β/α ratio with decreasing electric field strength. On the other hand, Ng *et al.* (2003) performed the photomultiplication measurement for thin 4H-SiC APD with extremely short illuminating light wavelength at 230nm to obtain pure hole-initiated multiplication. The author considers the effect of nonlocal impact ionization since dead space effect is significant in thin devices. They concluded that apart from pure hole-initiated multiplication, the inclusion of dead space does play an important role in reducing the excess noise factor. Liu *et al.* (2006) investigated the avalanche characteristics for 6H-SiC PIN APD with 0.25μm multiplication layer by using 325nm HeCd laser as the illuminating light. The device demonstrates a low excess noise factor ($k \approx 0.1$) with 9.2μA/cm^2 dark current density. The experimental work conducted by Rowland *et al.* (2009) examines the responsivity and dark current in 4H- and 6H-SiC APDs. The work shows that both device structures exhibits quite a similar behavior in the dark current measurement which increases rapidly near breakdown region. Recently, Zhou *et al.* (2011) studied the multiplication characteristics of SACM 4H-SiC APD with 0.25μm multiplication layer. A dark current density at 1.7μA/cm^2 is reported. However, the structure suffers a high excess noise factor at $k \approx 0.26$.

It can be noted that there is not much simulation work on the avalanche characteristics of APD had been carried out, especially for 6H-SiC. Most of the experimental results reported in the literature [8, 10 – 13] are mix carrier injection process, which in turn can caused a significant uncertainty towards the reported data. In this work, a detailed study on the avalanche characteristics of 4H- and 6H-SiC APDs at various avalanche widths are presented by using Monte Carlo (MC) model. The model utilizes random ionization path length (RIPL) with single electron or hole injection into the avalanche region for initiating the impact ionization. This model includes the effect of dead space that is the minimum distance that the carrier should travel in order to attain sufficient energy for impact ionization. This is an extension of the previous work which had been carried in the earlier stage [14 – 17].

RANDOM IONIZATION PATH LENGTH MODEL

This MC model considers two non-parabolic conduction bands and valence bands of the energy band structure. The scattering mechanisms considered are polar and non-polar optical phonon scattering, acoustic phonon scattering and impurity scattering. Impact ionization rate is computed based on the carrier energy that arises during the scattering processes. A modified Keldysh equation [14, 15] is used to model the impact ionization rate as a function of carrier energy in non-parabolic energy band structure. The energy related impact ionization rate is given as

$$\frac{1}{\tau^i(E)} = P_i\left(E - E_{th}^i\right)^{\gamma^i} \tag{1}$$

where i is the band index, P_i is the softness coefficient, E^i_{th} is the threshold energy and γ^i is the power exponent. Impact ionization coefficients are computed based on the number of times the carrier had scattered (n_e for electrons and n_h for holes) and the total distance they had travelled (l_{ei} for electrons and l_{hi} for holes) due to impact ionization in the momentum space. The reciprocal of averaging distance for these carriers yields the electron (α) and hole (β) impact ionization coefficients.

$$\alpha = \left[\sum_{i=1}^{n_e} l_{ei} \Big/ n_e\right]^{-1} \quad \text{cm}^{-1} \tag{2a}$$

$$\beta = \left[\sum_{i=1}^{n_h} l_{hi} \Big/ n_h\right]^{-1} \quad \text{cm}^{-1} \tag{2b}$$

Subsequently, the electric field dependent impact ionization coefficients equations of electron and hole have been deduced to ease the investigation of avalanche characteristics of APD. The general model for these equations are given as

$$\alpha = a_e \exp\left[-\left(\frac{E_c^e}{E}\right)^{\gamma^e}\right] \quad \text{cm}^{-1} \tag{3a}$$

$$\beta = a_h \exp\left[-\left(\frac{E_c^h}{E}\right)^{\gamma^h}\right] \quad \text{cm}^{-1} \tag{3b}$$

where E is the applied electric field. The value of each parameter for 4H- and 6H-SiC are listed in Table 1.

Table 1 The impact ionization coefficients parameters for 4H- and 6H-SiC.

Electron	a_e	E_c^e (V/cm)	γ^e
4H-SiC	1.803×10^6	1.352×10^7	1.20
6H-SiC	9.633×10^5	1.067×10^7	1.95

Hole	a_h	E_c^h (V/cm)	γ^h
4H-SiC	1.861×10^6	9.986×10^6	1.11
6H-SiC	5.439×10^5	4.850×10^6	1.63

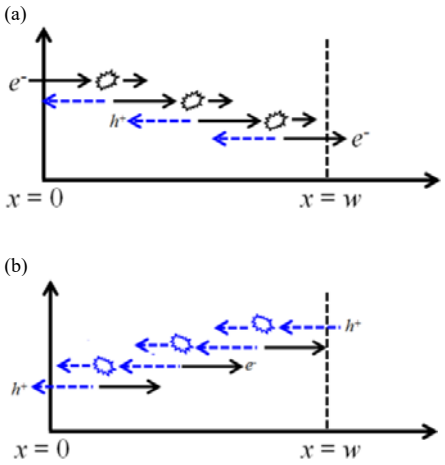

Fig. 1 (a) Injected electron at x = 0 for electron-initiated impact ionization for avalanche region x = 0 to x = w. (b) Injected hole at x = w for hole-initiated impact ionization for avalanche region x = 0 to x = w.

RIPL model is used for the simulation of multiplication gain and excess noise factor consider a single carrier injection into the avalanche region extending from x = 0 to x = w. From then on, both electrons and holes participate in the multiplication process under the effect of uniform high electric field ranging from 100kV/cm to 5MV/cm. As illustrated in Fig. 1(a), electron is injected at x = 0, and thereafter will travels in the positive x-direction throughout the avalanche region. Impact ionization occurs after the electron travels through a random distance (l_e), including the dead space. After each impact ionization event, a new electron-hole pair is created and results in a total of two electrons and one hole being generated in the avalanche region. These two electrons will travel in positive x-direction while the hole will travels in negative x-direction in the avalanche region for the next impact ionization.

Conversely, hole-initiated impact ionization as shown in Fig. 1(b) begins with a hole being injected at x = w which will travel in the negative x-direction in the avalanche region will impact ionize after the random distance, l_h. Subsequently, two holes which travel in negative x-direction and one electron which travels in positive x-direction are generated in the avalanche region. Impact ionization is completed after all carriers have left the avalanche region. The carrier random ionization path length in the avalanche region is determine from the random number (r) with the value between 0 and 1, written as

$$l_e = d_e - \frac{\ln(r)}{\alpha} \tag{4a}$$

$$l_h = d_h - \frac{\ln(r)}{\beta} \tag{4b}$$

where d_e and d_h are the dead space for electron and hole respectively. The impact ionization coefficients for electron and hole in 4H- and 6H-SiC determined by random ionization path lengths had been investigated in our previous work [17]. Based on the electric field dependent expressions of electron and hole impact ionization coefficients for these two polytypes, multiplication gain is then computed by taking the averaging of number of trials (n) up to 10^6 generated by a specific random number, r. The equations used for the calculation of multiplication gain, <M> and excess noise factor, F are given as follow

$$\langle M \rangle = \sum_{i=1}^{n} M_i \Big/ n \text{ and } F = \sum_{i=1}^{n} {M_i}^2 \Big/ n\langle M \rangle^2 \tag{5}$$

RESULTS AND DISCUSSION

Fig. 2 shows the impact ionization coefficients of 4H- and 6H-SiC obtained from our model. 4H-SiC has higher impact ionization coefficients than 6H-SiC owing to its wider energy band gap. However, both materials show that holes have higher impact ionization coefficients than that of electrons. Impact ionization coefficients increases with greater electric field strength since more impact ionization occurs in the avalanche region. The widely differing electron and hole impact ionization coefficients of these two materials are crucial in realizing high multiplication gain with low excess noise in APD.

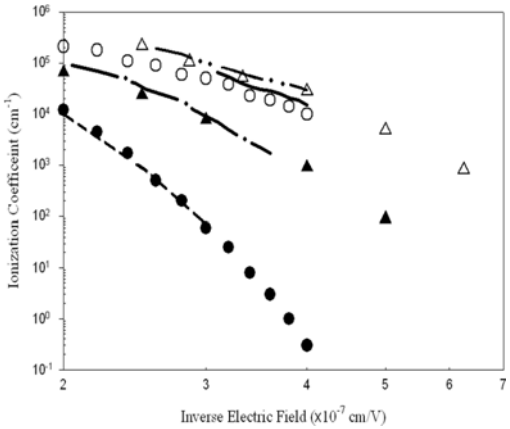

Fig. 2 Impact ionization coefficients for 4H-SiC (▲: electrons, Δ: holes) and 6H-SiC (●: electrons, ○: holes) obtained in this work. The results reported by Konstantinov et al. [18] (—●—: electrons, — ●●—: holes) for 4H-SiC, Ivanov et al. [19] (——: holes) and Hsing et al. [20] (— — —: electrons) for 6H-SiC are also shown.

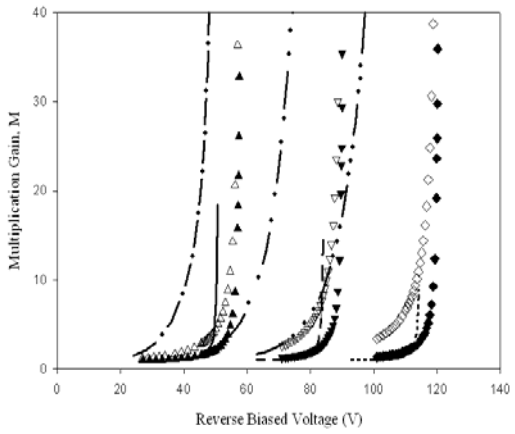

Fig. 3 4H- (symbols) and 6H-SiC (lines) APDs for electron-(▲,▼, ♦,——,— — and •••••) and hole-(Δ,▽, ◊, —•—, —••— and —•••—) initiated multiplication gain as a function of reverse-biased voltage with w = 0.1μm (▲, Δ,—— and —•—), 0.2μm (▼,▽,— — and —••—), and 0.3μm (♦,◊,••••• and —•••—).

The multiplication gain, breakdown voltage and excess noise factor for 4H- and 6H-SiC APDs in this work are observed at 0.1 μm, 0.2 μm and 0.3 μm avalanche widths. The multiplication gain and breakdown voltage obtained at each avalanche widths for 4H- and 6H-SiC APDs are presented in Fig. 3. Both 4H- and 6H-SiC APDs have high multiplication gain results from hole which increase with the thick avalanche width. Apparently, 4H-SiC APD experience a higher breakdown voltage than 6H-SiC APD at any avalanche width structure. This is mainly due to the wide energy band gap of 4H-SiC, which is at 3.23eV in comparable to 3.00eV of 6H-SiC. Besides that, 4H-SiC APD offers a higher multiplication gain near breakdown voltage than 6H-SiC APD. This benefit APD operating in Geiger-mode (GM), where the device is biased above breakdown voltage for a short interval for single photon detection [21, 22]. The characterization performance carried out by Bai *et al.* (2007) for 4H-SiC APD with quenching circuit shows a very low dark current at 59.5nA/cm^2 at a gain of 1000 in room temperature.

The excess noise factors of these two devices are presented in Fig. 4. Generally, both devices show a low excess noise factor arises from hole and it increases in thick avalanche structure. At w = 0.1 μm device length, hole-initiated process results in 4H-SiC APD has k = 0.3 while k = 0.37 for 6H-SiC APD. When the avalanche width is increased to 0.2 μm, k = 0.22 and k = 0.28 are observed for 4H- and 6H-SiC APD respectively. Whereas for w = 0.3 μm, 4H- and 6H-SiC APD has k = 0.18 and k = 0.22 respectively. For hole-initiated process, low k value indicates that more feedback electrons (thus more noise) are generated during impact ionization. As for electron-initiated process, low k value indicates that more forward electrons are generated during impact ionization. The electron-initiated process for both devices results in very high excess noise factor occurs at low multiplication gain. This had demerit electron as the initiating carrier for impact ionization. In overall, 4H-SiC APD experience a lower excess noise factor than 6H-SiC APD. This is mainly due to its high impact ionization coefficients as shown in Fig. 2.

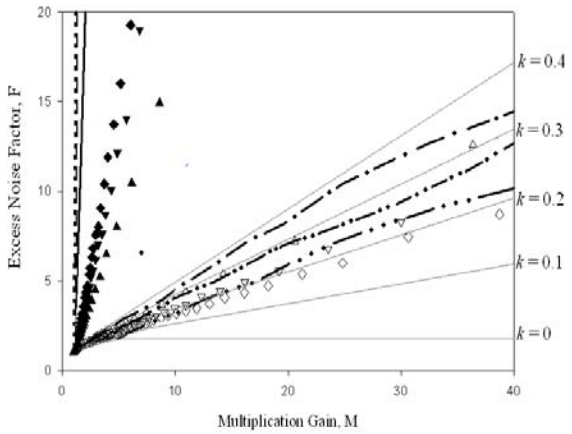

Fig. 4 4H- (symbols) and 6H-SiC (lines) APDs for electron- (▲,▼, ♦,——,— —and•••••) and hole- (Δ,▽, ◊, —•—,—••— and —•••—) initiated excess noise factor as a function of multiplication gain with w = 0.1μm (▲, Δ,—— and —•—), 0.2μm (▼,▽,— — and —••—), and 0.3μm (♦,◊,••••• and —•••—). Thin grey line indicates the k value for electron-initiated impact ionization calculated from McIntyre equation [23].

CONCLUSION

RIPL MC model with dead space effect is used to simulate the avalanche characteristics of thin 4H- and 6H-SiC APDs for avalanche widths at 0.1μm, 0.2μm and 0.3μm. Both devices observed a high multiplication gain and breakdown voltage at thick avalanche width. Besides that, hole-initiated impact ionization gives rise to a much higher multiplication gain than the electron-initiated impact ionization. 4H-SiC gives higher breakdown voltage than 6H-SiC due to its wider energy band gap at 3.23eV. Comparison of the simulated breakdown voltage and multiplication gain in this work is in a good agreement with those reported in the literature. Multiplication gain always associates with the presence of excess noise factor due to the stochastic process of impact ionization. This can cause a significant deterioration to the APD performance. For both 4H- and 6H-SiC APDs, holes produce much lower excess noise factor than electrons during impact ionization. Thus, in order to attain a high breakdown voltage with high multiplication gain, 4H-SiC should be the chosen material and hole should be selected as the initiating carrier for impact ionization in APD. This is in accordance to the high hole impact ionization coefficients achieved from previous MC model. Besides that, 4H-SiC APD has lower excess noise factor than 6H-SiC APD for hole impact ionization with identical avalanche width. Since a small k value is preferable as it indicates a low

excess noise factor, 4H-SiC is more preferable than 6H-SiC in APD design. This makes 4H-SiC to be more preferable than 6H-SiC not only in APD but also to other power devices design where high voltage application is needed.

ACKNOWLEDGEMENT

This work was supported by FRGS fund from Ministry of Higher Education, Malaysia.

REFERENCES

[1] F. Bertazzi, M. Moresco, E. Bellotti, J. Appl. Phys. 106 (2009) 063718.
[2] R. McClintock, J. L. Pau, C. Bayram, B. Fain, P. Giedraitis, M. Razeghi, M. P. Ulmer, in: Proc. SPIE 7222, 2009, p. 72220U1.
[3] M. Moresco, F. Bertazzi, E. Bellotti, IEEE J. Quantum Electron. 47 (2011) 447.
[4] J. C. Carrano, D. J. H. Lambert, C. J. Eiting, C. J. Collins, T. Li, S. Wang, B. Yang, A. L. Beck, J. C. Campbell, Appl. Phys. Lett. 76 (2000) 924.
[5] B. Giordanengo, A. Ben Moussa, J. F. Hochedez, A. Soltani, P. De Moor, K. Minoglou, P. Malinowski, J. Y. Duboz, Y. M. Chong, Y. S. Zou, W. J. Zhang, S. T. Lee, R. Dahal, J. Li., J. Y. Lin, H. X. Jiang, EAS Publ. Ser. 37 (2009) 199.
[6] J. C. Campbell, S. Demiguel, F. Ma, A. Beck, X. Guo, S. Wang, X. Zheng, X. Li, J. D. Beck, M. A. Kinch, A. Huntington, L. A. Coldren, J. Decobert, N. Tscherptner, IEEE J. Sel. Top. Quantum Electron. 10 (2004) 777.
[7] X. Guo, L. B. Rowland, G. T. Dunne, J. A. Fronheiser, P. M. Sandvik, A. L. Beck, J. C. Campbell, IEEE Photon. Tech. Lett. 18 (2006) 136.
[8] H. D. Liu, X. Y. Guo, D. McIntosh, J. C. Campbell, IEEE Photon. Tech. Lett. 18 (2006) 2508.
[9] J. P. R. David, C. H. Tan, IEEE J. Sel. Top. Quantum Electron. 14 (2008) 998.
[10] Q. Zhou, D. McIntosh, H. D. Liu, J. C. Campbell, IEEE Photon. Tech. Lett. 23 (2011) 299.
[11] W. S. Loh, B. K. Ng, S. I. Soloviev, H. Y. Cha, P. M. Sandvik, C. M. Johnson, J. P. R. David, IEEE Trans. Electron Devices 55 (2008) 1984.
[12] B. K. Ng, J. P. R. David, R. C. Tozer, G. J. Rees, F. Yan, J. H. Zhao, M. Weiner, IEEE Trans. Electron Devices 50 (2003) 1724.
[13] L. B. Rowland, J. L. Wyatt, J. Fronheiser, A. V. Vert, P. M. Sandvik, T. Borsa, B. Van Zeghbroeck, S. Babu, Mater. Sci. Forum 615 (2009) 869.
[14] C. C. Sun, A. H. You, E. K. Wong, AIP Conf. Proc. 1250, 2010, p. 281.
[15] C. C. Sun, A. H. You, E. K. Wong, AIP Conf. Proc. 1328, 2011, p. 277.
[16] C. C. Sun, A. H. You, E. K. Wong, 10th IEEE Int. Conf. Semicond. Electron. 2012, p. 366.
[17] C. C. Sun, A. H. You, E. K. Wong, Eur. Phys. J. Appl. Phys. 60 (2012) 10204.
[18] A. O. Konstantinov, Q. Wahab, N. Nordell, U. Lindefelt, Appl. Phys. Lett. 71 (1997) 90.
[19] P. A. Ivanov, V. E. Chelnokov, Semicond. Sci. Tech. 7 (1992) 863.
[20] E. H. S. Hsing, J. F. Gray, Microelectron. J. 30 (1999) 1.
[21] X. Bai, D. Mcintosh, H. Liu, J. C. Campbell, IEEE Photon. Tech. Lett. 19 (2007) 1822.
[22] A. L. Beck, G. Karve, S. Wang, J. Ming, X. Guo, J. C. Campbell, IEEE Photon. Tech. Lett. 17 (2005) 1507.
[23] R. J. McIntyre, IEEE Trans. Electron Devices ED-13 (1966) 164.